arXiv:1401.0455v1 [astro-ph.GA] 2 Jan 2014

To appear in AJ

SMA Submillimeter Observations of HL Tau: Revealing a compact molecular outflow

Alba M. Lumbreras,[1,2] and Luis A. Zapata[1]

ABSTRACT

We present archival high angular resolution ($\sim 2''$) ^{12}CO(3-2) line and continuum submillimeter observations of the young stellar object HL Tau made with the Submillimeter Array (SMA). The ^{12}CO(3-2) line observations reveal the presence of a compact and wide opening angle bipolar outflow with a northeast and southwest orientation (P.A. = 50°), and that is associated with the optical and infrared jet emanating from HL Tau with a similar orientation. On the other hand, the 850 μm continuum emission observations exhibit a strong and compact source in the position of HL Tau that has a spatial size of $\sim 200 \times 70$ AU with a P.A. = 145°, and a dust mass of around 0.1 $M_\odot$. These physical parameters are in agreement with values obtained recently from millimeter observations. This submillimeter source is therefore related with the disk surrounding HL Tau.

Subject headings: ISM: Jets and outflows; Stars: Pre-main sequence; Stars: Mass loss

1. Introduction

HL Tau is a young star of solar-type located in the Taurus molecular cloud, a close-by star-forming region at a distance of about 140 pc (Torres et al. 2007; Rebull et al. 2004). This young star has been extensively studied at many wavelengths, some of these include radio, millimeter, infrared, and optical (Mundy et al. 1996; Wilner et al. 1996; Anglada et al. 2007; Takami et al. 2007; Krist et al. 2008; Carrasco-González et al. 2009; Kwon et al. 2011). These observations have revealed that HL Tau possesses yet a well defined disk-outflow

[1]Centro de Radioastronomía y Astrofísica, UNAM, México.

[2]Benemérita Universidad Autónoma de Puebla, Puebla, México

system. The circumstellar disk has a mass of 0.13 $M_{\odot}$, a characteristic radius of 80 AU, and a position angle P.A. = 136° (Kwon et al. 2011). On the other hand, the infrared and optical observations show the presence of a collimated jet emanating from HL Tau with an orientation northeast and southwest (P.A. = 50°; Krist et al. 2008). At very small scales ($\sim$ 50 AU) a radio thermal jet has also been reported to be associated with HL Tau with a similar orientation to that shown by the optical and infrared jet (Rodríguez et al. 1994; Carrasco-González et al. 2009). Robitaille et al. (2007) confirmed that HL Tau has a large dusty envelope discovered through modeling to a spectral energy distribution over different frequencies. This envelope was reported for the first time by Cabrit et al. (1996).

At large scales ($\sim$ 2000 AU), using single dish millimeter telescopes, Monin et al. (1996); Cabrit et al. (1996) found a very extended northeast and southwest molecular outflow emanating from HL Tau. This flow was reported as an anisotropic, mostly redshifted that is emanating from within a flattened molecular remnant envelope. Cabrit et al. (1996) also showed Plateau de Bure interferometer (PdBI) maps that revealed small-scale structures nested in the putative extended molecular outflow.

Here, we present submillimeter observations that reveal a very well defined molecular compact and wide opening angle bipolar outflow with a northeast and southwest orientation that is likely associated with the large-scale monopolar molecular outflow reported by Monin et al. (1996); Cabrit et al. (1996). The 850 μm continuum images reveal that the dust emission at this wavelength is mainly associated with its circumstellar disk.

2. Observations

The observations were obtained from the SMA archive, and were collected on October 2005, when the array was in its compact configuration. The 21 independent baselines in the compact configuration ranged in projected length from 13 to 79 kλ. The phase reference center for the observations was at $\alpha_{J2000.0} = 04^{\rm h}31^{\rm m}38\overset{\rm s}{.}41$, $\delta_{J2000.0} = +18°13'57\overset{''}{.}79$. Two frequency bands, centered at 336.5 GHz (Lower Sideband) and 346.5 GHz (Upper Sideband) were observed simultaneously. The primary beam of the SMA at 345 GHz has a FWHM $\sim 30''$. The submillimeter emission arising from HL Tau falls very well inside of the FWHM.

The SMA digital correlator was configured in 24 spectral windows ("chunks") of 104 MHz and 128 channels each. This provides a spectral resolution of 0.815 MHz ($\sim$ 0.7 km s^{-1}) per channel. The system temperatures (T_{DSB}) varied in a range of 200 to 450 K, indicating good weather conditions. Observations of Uranus provided the absolute scale for the flux calibration. The gain calibrator was the quasar 3C 111, while Uranus was also used for

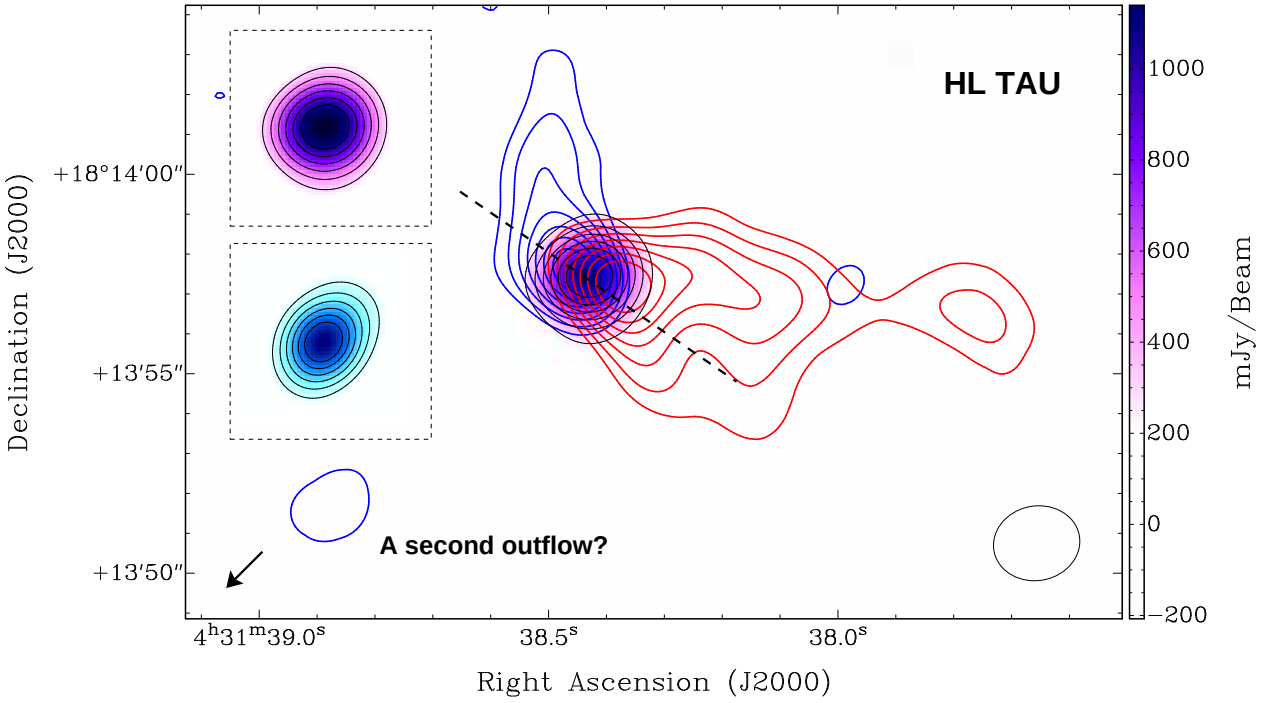

Fig. 1.— High-velocity SMA integrated intensity (moment 0) contour (blue and red) map of the ^{12}CO(3-2) thermal emission, and the continuum emission at 850 μm (yellow scale and black contours) from HL Tau. The blue contours represent blueshifted gas, while the red contours represent redshifted gas. The blue and red contours range from, 30% to 90% of the peak emission, in steps of 10%. The emission peaks for the blueshifted and redshifted emission are 6.5 and 19.1 Jy Beam^{-1} km s^{-1}, respectively. The black contours range from 35% to 90% of the peak emission, in steps of 10%. The peak of the continuum emission is 1.0 Jy beam^{-1}. The synthesized beam of the continuum image is shown in the lower right corner. The dashed black line with a P.A. of 50° traces the position where the position-velocity diagram shown in Figure 3 was computed. The black arrow marks the orientation of a possible second outflow emanating from HL Tau. The CO synthesized beam is very similar to that of the continuum image, see text. We show in the upper left corner the continuum source (purple scale) and the resulting continuum source (blue scale) after restoring it with a beam size slightly smaller of 1.″7 × 1.″7 with a P.A. = +85°. For the blue scale image, the contouring is the same as above but with the peak at 0.6 Jy Beam^{-1}. The negative contours are not shown in this image.

bandpass calibration. The uncertainty in the flux scale is estimated to be between 15 and 20%, based on the SMA monitoring of quasars. Further technical descriptions of the SMA can be found in Ho et al. (2004).

The data were calibrated using the IDL superset MIR, originally developed for the

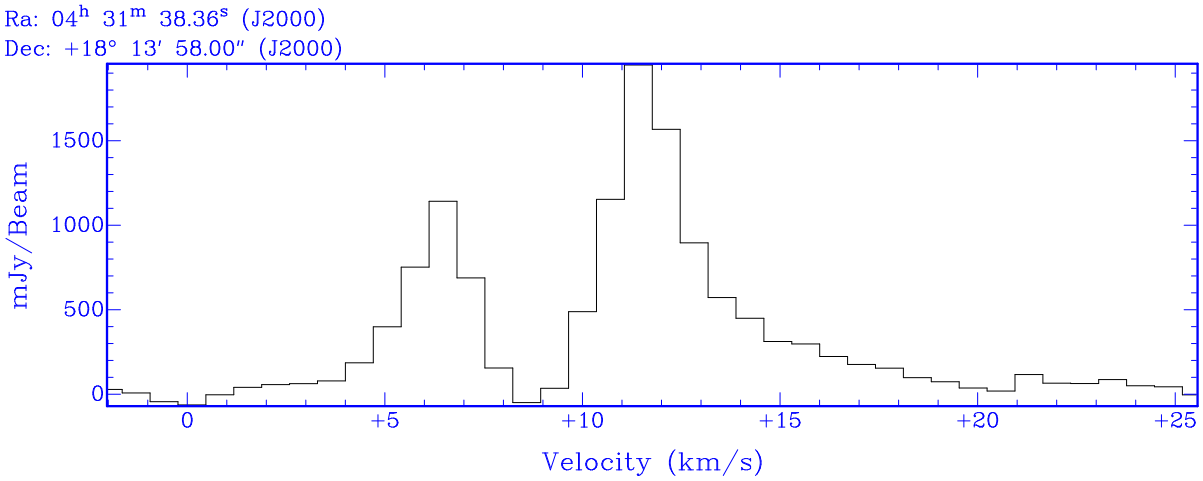

Fig. 2.— Average spectra of the ^{12}CO(3-2) line towards HL Tau. On top of the image is shown the central position of the box, where the spectra was obtained. The spectra was obtained from an area delimited by a 5" × 5" square. The velocity here is LSR.

Owens Valley Radio Observatory (OVRO, Scoville et al. 1993) and adapted for the SMA.[1] The calibrated data were then imaged and analyzed in the standard manner using the MIRIAD and KARMA (Gooch 1996; Sault et al. 1995) softwares. A 850 μm continuum image was obtained by averaging line-free channels in the upper sideband with a total bandwidth of 2 GHz. For the line emission, the continuum was also removed. The ^{12}CO(3-2) was the only spectral line detected. For the continuum emission, we set the *R*OBUST parameter of the task *I*NVERT to -2 to obtain a slightly higher angular resolution allowing us to obtain a better fitting for the size of HL Tau, while for the line emission we set this to +2 in order to obtain a better sensitivity sacrificing angular resolution.

The resulting r.m.s. noise for the continuum image was about 20 mJy beam^{-1} at an angular resolution of $2\farcs07 \times 1\farcs88$ with a P.A. = +85.2°. The r.m.s. noise in each channel of the spectral line data was about 200 mJy beam^{-1} at an angular resolution of $2\farcs38 \times 2\farcs19$ with a P.A. = +14.5°.

[1]The MIR-IDL cookbook by C. Qi can be found at http://cfa-www.harvard.edu/~cqi/mircook.html.

3. Results

3.1. Continuum emission

In Figure 1, we show the resulting 850 μm continuum image from HL Tau made with the SMA. We only detected a single source that is associated with HL Tau. This source has a position in the sky of $\alpha_{J2000.0} = 04^{\rm h}31^{\rm m}38\overset{\rm s}{.}42$, $\delta_{J2000.0} = +18^{\circ}13'57\overset{''}{.}39$, with a positional error of less than $1\overset{''}{.}0$. This position coincides very well within the uncertainty with the position obtained by Mundy et al. (1996) at 2.7 mm with BIMA, discarding any proper motion of HL Tau in this interval of time.

We measured a flux density and peak intensity for this compact source of 1.3±0.3 Jy and 1.0±0.2 Jy Beam^{-1}, respectively. These flux values are in good agreement with the SED for HL Tau obtained in Kwon et al. (2011). In Figure 1, HL Tau looks something rounded, however, this is resolved as an elongated source using the task of MIRIAD *imfit* and *jmfit* of AIPS. These two tasks use elliptical gaussian fittings to estimate the source parameters. The deconvolved size that we get is that one for an elongated source with a northwest-southeast orientation (approximately $1\overset{''}{.}5 \times 0\overset{''}{.}5$ with a P.A. = +145°). This angular size corresponds to $\sim 200 \times 70$ AU with a P.A. = 145° at the distance of the Taurus molecular cloud. These size values also are in good agreement with those values already obtained by Kwon et al. (2011) using CARMA 1.3 and 2.7 mm observations. Given the high signal-to-noise ratio obtained from our observations, we tried to verify the results obtained by the tasks *imfit* and *jmfit*, and we then restored our original image with a slightly smaller beam (see Figure 1) revealing the elongated morphology obtained by the tasks.

Assuming optically thin isothermal dust emission, a gas-to-dust ratio of 100, a dust temperature of 30 K, a dust mass opacity $\kappa_{850\mu{\rm m}} = 1.5$ cm^2 g^{-1}, and an emissivity index $\beta = 1.0$, (see Mundy et al. 1996; Kwon et al. 2011), we estimate roughly a total mass for the source of 0.1±0.02 $M_\odot$. The uncertainty here is only the error in the flux measurement of HL Tau. However, we noted that the temperature for the disk used here could be higher as shown in the model presented in Kwon et al. (2011).

This combination of properties suggest that the emission seen at 850 μm is dominated by the accretion disk, although a very small contribution from the inner envelope might also be present.

3.2. ^{12}CO(3-2) line emission

In Figure 2, we show the average spectrum of the ^{12}CO(3-2) line towards HL Tau. The box length of the averaging spectra is about 5 arcseconds centered in the position of HL Tau. The spectrum has two strong peaks, the first peak of the spectrum appears to be at a velocity slightly smaller than 6.5 km/s, and the other one about 11.5 km s^{-1}. The systemic velocity of the cloud is $\sim$ 6.5 km/s (Monin et al. 1996 and Cabrit et al. 1996). The blueshifted peak is probably arising from the outflow and disk as revealed by Cabrit et al. (1996). The blueshifted peak is fainter than the redshifted one. There is one dip feature about 8.5 km s^{-1}, maybe caused for the missing flux at velocities close to the systemic. In addition, there are some faint high velocity features associated with the outflow emanating from HL Tau.

In Figure 1, additionally to the 850 μm continuum image, we have overlaid the integrated intensity (moment 0) high-velocity map of the ^{12}CO(3-2) thermal emission. In the image the blue and red colors correspond to the blueshifted and redshifted gas emission, respectively. To construct the moment 0 high-velocity maps, we have integrated LSR velocities ranging from +1.88 km s^{-1} to +5.1 km s^{-1} for the blue shifted one, and LSR velocities ranging from +13.24 km s^{-1} to +25.53 km s^{-1} for the redshifted. The emission at ambient velocities (+6 to +11 km s^{-1}) was clearly extended and poorly sampled with the SMA, and was suppressed in this moment zero map. This extended emission is arising mainly from the molecular cloud, and thus the systemic velocity of the cloud and HL Tau should be placed within this range.

This image reveals a compact bipolar molecular outflow emanating from HL Tau. The bipolar outflow has a northeast and southwest axis with a position angle of about 50°. We thus noted that this bipolar outflow is the molecular counterpart of the optical and infrared jet that emanates from HL Tau with a similar position angle (Anglada et al. 2007; Takami et al. 2007; Krist et al. 2008). However, contrary of being collimated as the optical and infrared jet, and other bipolar molecular outflows *e.g.* HH 797 or HH 625 (Zapata et al. 2005; Pech et al. 2012), the molecular counterpart is a wide opening angle outflow and is only present very close to HL Tau. These physical properties have also been observed in other outflows, for example, in the HH 30, and are attributed to the entrainment by the optical jet (Pety et al. 2006).

We note that both the blue and red northwest walls appear to be significantly more defined than the southeast ones. A possibility is that this effect could be created if very dense molecular material is present in the west part of the cloud. This condition will help to a better entrainment of the molecular gas material.

The spatial structure of the moderate/low velocity gas of the bipolar outflow as a function of the radial velocities (position-velocity diagram) along the mayor axis is shown in

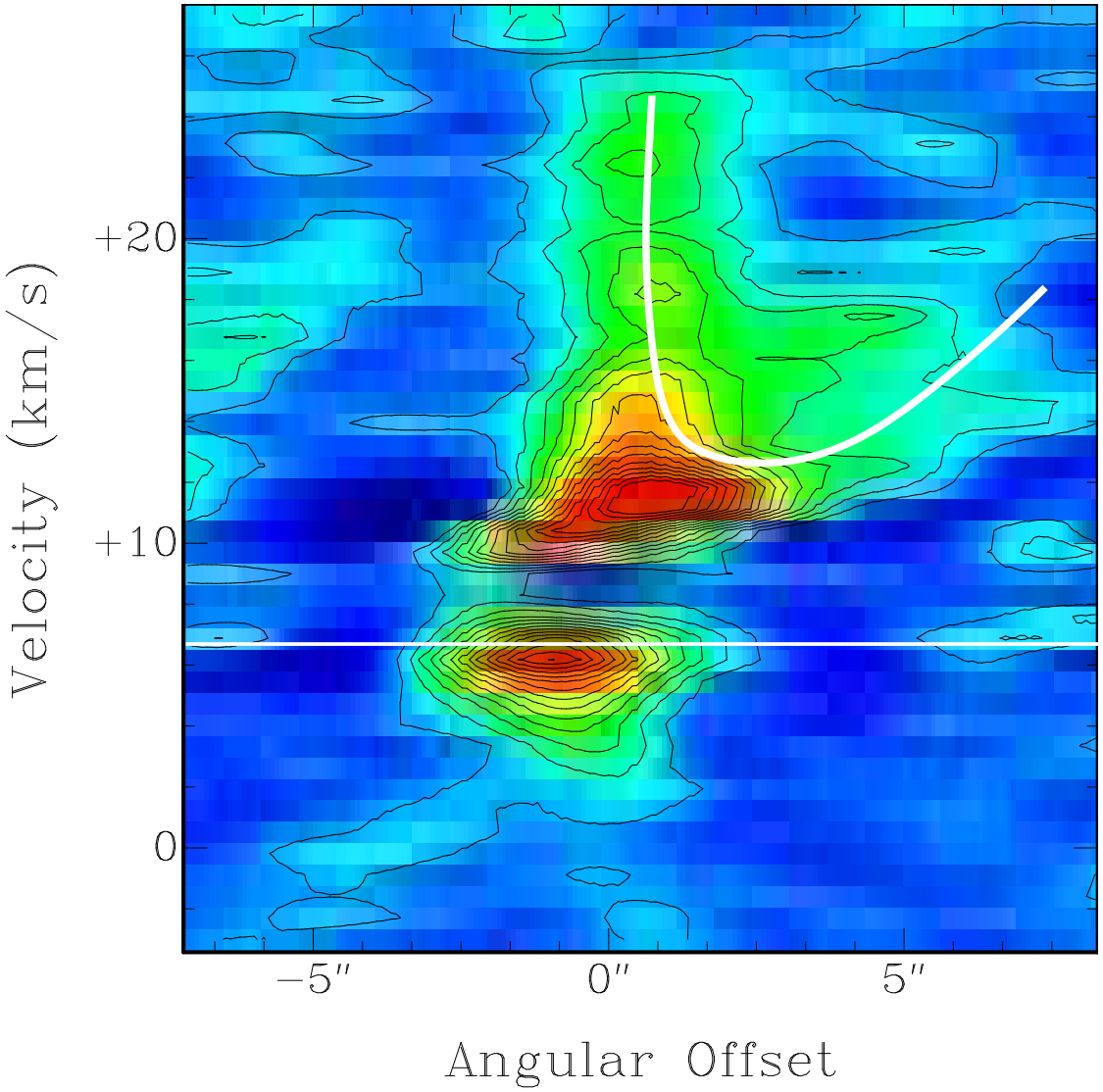

Fig. 3.— Position-velocity diagram of the CO outflow computed at a position angle of +50°. The contours range from 20% to 90% of the peak emission, in steps of 5%. The peak of the line emission is 6.5 Jy beam^{-1}. The systemic LSR radial velocity of the ambient molecular cloud is about +6.5 km s^{-1} and is represented with a straight line. The synthesized beam is 2.38″ × 2.19″ with a P.A. of +14.5°, and the spectral resolution is ∼ 0.7 km s^{-1}. The white curved line illustrates the wide-angle feature observed in its redshifted side. The negative contours are not shown in this image.

Figure 3. This image shows how the redshifted component covers a much wider range of velocities than the blueshifted side. The redshifted lobe displays a high velocity component with a low-velocity component extending far from the position of the star. On the other hand, the blue side of the outflow displays only a limited range of velocities close to the exciting source.

Based on Figures presented by Arce et al. (2007); Lee et al. (2000) that show the molec-

ular outflow properties predicted by different models, and in the morphology and the PV diagram obtained here from the outflow (Figures 1 and 3), we suggest that this outflow is reminiscent of a wide-angle outflow. However, we noted that there is also a collimated jet emanating simultaneously from HL Tau mapped in the optical and infrared wavelengths (Krist et al. 2008). This is therefore one of the outflows that seems to present simultaneously a jet and a wide-angle outflow (see Arce et al. 2007). However, many more sensitive high-angular resolution observations are needed to resolve better the putative wide-angle outflow and the jet.

Assuming that we are in local thermodynamic equilibrium (LTE), that the ^{12}CO(3-2) molecular emission is optically thin, a fractional abundance between the carbon monoxide and the molecular hydrogen of 10^4, a distance of 140 pc, an excitation temperature T_{ex} = 50 K, we estimated a mass for the outflow energized by HL Tau of 2.5 $\times$ 10^{-3} $M_\odot$. This value for the outflow mass is expected for a flow energized by a young low-mass protostar, see Wu et al. (2004). The uncertainty in the outflow mass is on the order of a factor of two, mainly due to the ambiguity of the excitation temperature. We also estimate a kinematical energy of 3 $\times$ 10^{42} ergs, an outflow momentum of 0.03 $M_\odot$ km s^{-1}. These estimates do not take into consideration the inclination of the outflow with respect to the line-of-sight and the amplitude calibration.

We found some faint molecular emission toward the southeast of HL Tau (about 10″), where is located the optical object HH 153, see Figure 1. The emission revealed in Figure 1 seems to be marginal, however this emission is present in a few velocity channels (−0.88 to +1.24 km s^{-1}) making more reliable our detection. The HH 153 is a traverse outflow that appears to emanate from the HL Tau vicinity (Krist et al. 2008). However, we note that the measured proper motions of HH 153 (knots Halpha-B1, B2, B3, C1, C2; Anglada et al. 2007) point away from HL Tau supporting also an origin in this source. Future sensitive molecular observations of this region may help in revealing its energizing object.

4. Conclusions

We have observed in the submillimeter regime the young star HL Tau using the Submillimeter Array. Our conclusions are as follow:

- The ^{12}CO(3-2) line observations reveal the presence of a compact and wide opening angle bipolar outflow with a northeast and southwest orientation (P.A. = 50°), and that is associated with the optical and infrared jet emanating from HL Tau with a similar orientation. The compact outflow has a mass of about 2.5 $\times$ 10^{-3} $M_\odot$.

- We found that in the redshifted side of the outflow there is evidence of a wide-angle outflow that probably is associated with an optical jet. This outflow is likely associated with the large-scale monopolar molecular outflow reported by Monin et al. (1996); Cabrit et al. (1996).
- The 850 μm continuum emission observations show a strong and compact source in the position of HL Tau itself that has a deconvolved size of $\sim 200 \times 70$ AU with a P.A. $= 145^{\circ}$ and a mass of 0.1 $M_{\odot}$.

L.A.Z. acknowledge the financial support from DGAPA, UNAM, and CONACyT, México. We would like to thank to the anonymous referee for the comments, which definitively help to improve our manuscript.

Facilities: SMA.

REFERENCES

Anglada, G., López, R., Estalella, R., et al. 2007, AJ, 133, 2799

Arce, H. G., Shepherd, D., Gueth, F., et al. 2007, Protostars and Planets V, 245

Cabrit, S., Guilloteau, S., Andre, P., et al. 1996, A&A, 305, 527

Carrasco-González, C., Rodríguez, L. F., Anglada, G., & Curiel, S. 2009, ApJ, 693, L86

Gooch, R. 1996, Astronomical Data Analysis Software and Systems V, 101, 80

Ho, P. T. P., Moran, J. M., & Lo, K. Y. 2004, ApJ, 616, L1

Krist, J. E., Stapelfeldt, K. R., Hester, J. J., et al. 2008, AJ, 136, 1980

Kwon, W., Looney, L. W., & Mundy, L. G. 2011, ApJ, 741, 3

Lee, C.-F., Mundy, L. G., Reipurth, B., Ostriker, E. C., & Stone, J. M. 2000, ApJ, 542, 925

Mundy, L. G., Looney, L. W., Erickson, W., et al. 1996, ApJ, 464, L169

Monin, J.-L., Pudritz, R. E., & Lazareff, B. 1996, A&A, 305, 572

Pech, G., Zapata, L. A., Loinard, L., & Rodríguez, L. F. 2012, ApJ, 751, 78

Pety, J., Gueth, F., Guilloteau, S., & Dutrey, A. 2006, A&A, 458, 841

Rebull, L. M., Wolff, S. C., & Strom, S. E. 2004, AJ, 127, 1029

Robitaille, T. P., Whitney, B. A., Indebetouw, R., & Wood, K. 2007, ApJS, 169, 328

Rodriguez, L. F., Canto, J., Torrelles, J. M., et al. 1994, ApJ, 427, L103

Sault, R. J., Teuben, P. J., & Wright, M. C. H. 1995, Astronomical Data Analysis Software and Systems IV, 77, 433

Scoville, N. Z., Carlstrom, J. E., Chandler, C. J., et al. 1993, PASP, 105, 1482

Takami, M., Beck, T. L., Pyo, T.-S., McGregor, P., & Davis, C. 2007, ApJ, 670, L33

Torres, R. M., Loinard, L., Mioduszewski, A. J., & Rodríguez, L. F. 2007, ApJ, 671, 1813

Wilner, D. J., Ho, P. T. P., & Rodriguez, L. F. 1996, ApJ, 470, L117

Wu, Y., Wei, Y., Zhao, M., et al. 2004, A&A, 426, 503

Zapata, L. A., Rodríguez, L. F., Ho, P. T. P., et al. 2005, ApJ, 630, L85

This preprint was prepared with the AAS LaTeX macros v5.2.